Published in final edited form as:
Psychiatry Res. 2013 April 30; 212(1): 1–6. doi:10.1016/j.pscychresns.2012.10.012.

Quantitative morphology of the corpus callosum in obsessive–compulsive disorder

Katherine C. Lopez, **Francois Lalonde**, **Anand Mattai**, **Benjamin Wade**, **Liv Clasen**, **Judith Rapoport**, and **Jay N. Giedd***
Child Psychiatry Branch, National Institute of Mental Health, National Institutes of Health, Building 10, Room 4C110, 10 Center Drive, MSC 1367, Bethesda, MD, USA

Abstract

Neuroimaging studies have implicated the corpus callosum (CC) in the pathophysiology of obsessive-compulsive disorder (OCD). Putative dysfunctions in prefrontal cortical regions suggest anomalies in anterior segments of the CC. However, recent studies have also implicated the middle and posterior CC. The present study soughts to examine the CC using parcellation scheme informed by diffusion tensor imaging. Anatomic brain magnetic resonance scans were obtained from 21 OCD subjects (mean age = 26.9±9.93) and 42 healthy age- and sex-matched controls (mean age = 26.6±9.46) between the ages of 14 and 49. Area and volume measures of five subregions of the CC were obtained via manual tracings. A multivariate analysis of variance (after correcting for multiple comparisons) identified smaller area and volume in the mid-anterior region of the CC in OCD patients relative to controls. These findings implicate medio-frontal regions of the cortex in the pathophysiology of OCD.

Keywords

Obsessive–compulsive disorder; Corpus callosum; Morphometry; Magnetic resonance imaging

1. Introduction

Obsessive–compulsive disorder (OCD) has a lifetime prevalence of approximately 2% (Fontenelle et al., 2006) and is characterized by the following: (1) intrusive and unwanted thoughts, beliefs, or ideas that cause significant distress and anxiety (i.e. obsessions) and (2) ritualistic or repetitive actions intended to subdue the anxious obsessions (i.e. compulsions). Neuroimaging studies have implicated frontal–striatal circuitry in the pathophysiology of OCD, with reports of structural and functional abnormalities in the prefrontal cortex (Szeszko et al., 1999; Kang et al., 2004; Friedlander and Desrocher, 2006; Baxter et al., 1988; Nordahl et al., 1989), basal ganglia (Szeszko et al., 1999; Scarone et al., 1992), and corpus callosum (CC) (Rosenberg et al., 1997).

*Corresponding author. Tel.: +301 435 4517; fax: +301 480 8898. jg@mail.nih.gov (J.N. Giedd). .

1.1. Corpus callosum

The CC is composed of ~200 million, mostly myelinated axons that connect homologous areas of the left and right cerebral cortex. Its relative ease of quantification on magnetic resonance imaging (MRI) and its central role in interhemispheric communication have made the CC a frequent target for neuroimaging investigations of several disorders, including OCD (Rosenberg et al., 1997). As fibers generally connect via the shortest route, the CC maintains a roughly topographic representation of the cortex (Hofer and Frahm, 2006; Fabri et al., 2010). Different methods have been proposed to divide the CC into segments corresponding to functionally distinct cortical regions from which the interhemispheric axons arise. Parcellation schemes include those devised by Weis (1991), Witelson (1989), Seltzer et al. (1986), and Hofer and Frahm (2006).

Weis subdivided the CC into five equal segments relative to the total CC length. Witelson and Seltzer took a more functional approach, dividing the CC into five vertical regions based on postmortem measures and autoradiograms (injections of radiolabelled amino acid) of rhesus monkeys. In the most widely used scheme, Witelson (1989) divided the CC into (1) an anterior third (CC1), comprising the rostum, genu, and rostral body, which projects to prefrontal, premotor and supplementary motor cortices; (2) a middle third, including the mid-anterior (CC2) and mid-posterior (CC3) bodies, proposed to extend to anterior and posterior parietal cortices, respectively; and (3) a posterior third, including the isthmus (CC4) and splenium (CC5), which extends to posterior parietal, temporal, and occipital cortices. More recently, Hofer and Frahm (2006) established a variation of Witelson's scheme using in vivo fiber tractography through diffusion tensor imaging (DTI), wherein the segmentation of the CC is based on topographical white matter projections to the cortex. The Hofer-Frahm scheme is suggested to provide a more accurate representation of human cortical–callosal connectivity than the earlier animal-informed parameters.

1.2. Callosal pathology in OCD

A typical connectivity in axons linking prefrontal cortices to frontal regions of CC (Yoo et al., 2007; Li et al., 2011; Bora et al., 2011; Menzies et al., 2008; Oh et al., 2012) suggests abnormalities in the anterior-most segment of the CC. Several reports of CC1 pathology support this hypothesis. In two DTI studies, both Saito et al. (2008) and Nakamae et al. (2011) localized white matter abnormalities in CC1. MacMaster et al. (1999) found similar results using signal intensity, wherein drug-free OCD patients showed decreased signal intensity in CC1, specifically in the anterior genu. Among the few structural imaging studies that functionally examined the CC, Rosenberg et al. (1997) identified increased area in CC1 in addition to middle and posterior CC abnormalities.

An increasing number of studies also found middle and posterior abnormalities, suggesting that callosal pathology may not be restricted to anterior regions of the CC. In a recent DTI study, Li et al. (2011) identified white matter abnormalities along the body of the CC in addition to the genu. Bora et al. (2011) also used DTI and detected decreased fractional anisotropy in the body of the CC including mid-regions. Using DTI, both Zarei et al. (2011) and Garibotto et al. (2010) found abnormal connectivity in the CC5 (i.e., splenium) in OCD patients. Studies using structural imaging have identified similar findings. While Rosenberg

et al. (1997) found increased area in CC5 in addition to frontal and middle sectors, Park et al. (2010) identified isolated posterior CC enlargements suggesting possible dysfunction in parietotemporal and occipital cortices. While these findings (see Table 1 for summary) implicate middle and posterior CC as regions of pathology, reports have been inconsistent.

Differences in CC segmentation may drive these regional CC inconsistencies. These discrepancies may be especially prominent in mid-regions where topographic parameters to the cortex are most variable across schemes. Thus, callosal segmentation may not only present variability in detecting regional pathology of the CC but also in ascertaining anatomical connectivity to the cortex.

Most studies have employed Witelson's animal-informed parcellation model to study human cortico–callosal relationships. Only recently have a few DTI studies adopted Hofer–Frahm guidelines to examine the CC in OCD (Li et al., 2011; Garibotto et al., 2010). To our knowledge, there are no existing studies that have applied these parameters to structural measures of the CC. Furthermore, studies have utilized length, area, and thickness as measures of CC structure but have not examined volume. Obtaining a three-dimensional measure of structure may afford a more comprehensive insight into regional differences of CC morphology. The present study sought to apply the Hofer-Frahm parameters to area and volume measurements of the CC to examine whether structural abnormalities are present in middle and posterior regions of the CC, as suggested by recent reports.

2. Methods

2.1. Participants

Adults exhibiting obsessive–compulsive symptoms were sought through national recruitment between 1991 and 1997. Participants were screened and tested at the Bethesda campus of the National Institutes of Health (NIH). Twentyone patients ranging from ages 14 to 49 (Mean age = 26.9±9.93) met the DSM-III criteria for OCD and were included in the study's sample.

Severity of diagnosis was assessed through a series of scales measuring the extent of preoccupation with obsessions or rituals, impediment in normal functioning, time spent on ritual behaviors, and the level of overall anxiety. The scales utilized include the Yale-Brown Obsessive–Compulsive Scale, Obsessive–Compulsive Rating Scale, National Institute of Mental Health Global OCD Rating Scale, and the Comprehensive Psychopathological Rating Scale–OCD subscale. Furthermore, all patients underwent laboratory testing, neurological assessments, and a physical exam to ascertain overall health. Participation in the study required a 4 week abstinence from psychotropic drugs. See Table 2 for characteristics of our clinical group.

Forty-two healthy controls (mean age = 26.6±9.46) were sex- and age-matched to psychiatric patients at a 2:1 ratio. Controls were recruited as part of an ongoing longitudinal study on typical brain development at the National Institute of Mental Health. Participation in the study required the completion of a battery of neuropsychological assessments and both physical and neurological examinations. Participants with current or past psychiatric

diagnosis, history of drug or alcohol abuse and any medical condition affecting brain development were excluded.

IQ scores were obtained from all participants using either the Wechsler Adult Intelligence Scale (WAIS) or the Wechsler Abbreviated Scale of Intelligence (WASI). Participants signed informed consent regarding the nature of the study, procedures involved, and potential risks.

2.2. MRI acquisition

All subjects were scanned at the NIH using a Bethesda, Maryland using a 1.5 T GE Sigma scanner. High-resolution MRI scans were acquired using a three-dimensional spoiled gradient-recalled pulse sequence to obtain T1-weighted axial whole brain images with a 1.5 -mm slice thickness and an in-plane resolution of 0.9375 by 0.9375 mm. Pulse parameters were selected to maximize gray and white matter tissue contrast and consisted of the following: repetition time: 24 ms; echo time: 5 ms; flip angle: 45°; matrix: 256 × 192; number of excitations: 1; field of view: 24 cm; acquisition time: 9 min, 52 s. A dual echo fast spin echo scan was also acquired to collect T2-weighted and proton density images for clinical evaluation.

2.3. Corpus callosum measurement

The Medical Image Processing, Analysis and Visualization tool (http://mipav.cit.nih.gov) was used to manually trace and measure the CC. Images were aligned to standard orientation using a rigid-body rotation. The brain images were rotated in the axial plane so that the interhemispheric fissure was parallel to the *y*-axis. In the sagittal plane, images were rotated so that the line segment connecting the furthest anterior and posterior points of the CC was parallel to the *x*-axis. The mid-sagittal slice, used to obtain area measurements, was chosen as the slice that contained the maximum curvature of the rostrum or contained the most visible septum pellucidum. Binary images of the CC were made for five sagittal slices with the mid-sagittal as the center slice. Binary segmentation was a semi-automated procedure with manual adjustments made by a rater (KL) who was unaware of diagnosis. The five binary slices were divided into five subdivisions using an in-house MATLAB program. First, the anterior–posterior length of the CC mask was found. Then each voxel was assigned to a subdivision based on relative anterior–posterior location according to the proportions proposed by Hofer and Frahm (2006). If a voxel on the border of two subdivisions would have been classified as a mixture of two subdivisions, it was classified as the subdivision with the highest proportion. If both were equally represented, then it was classified as the more anterior region. After segmentation, the volume of each CC subdivision was summed across all slices. During training the rater (KL) demonstrated high inter-rater reliability with one other rater (intraclass correlation coefficients=0.92). Intra-rater reliabilities for the study were determined from repeated measurement in separate sessions of 60 randomly selected scans, blind to prior measurement. Intraclass correlation coefficients were high, with averaged ICC=0.94 for all five regions. Parcellation of the CC as performed by manual tracings is depicted in Fig. 1. For regions traced, see Table 3.

2.4. Statistical analysis

CC measurements for both area and volume were analyzed using a multivariate analysis of variance (MANOVA) that included the five regions of the CC as dependent variables, diagnosis as the grouping variable, with age and sex as covariates. Contrasts for each region were performed and significance thresholds were adjusted for multiple comparisons using a Bonferroni correction. Due to our small sample size, we calculated the effect size for each CC segment found to be statistically significant.

3. Results

3.1. Area

MANOVA results yielded significant group differences for the overall model (Wilk's Lambda, $F = 2.48$, $p = 0.043$) with no significant age or sex effects. Bonferroni-corrected individual region contrasts were significant only for region 2 (F=4.62, p=0.036) and region 5 (F=4.83, p=0.032). The effect sizes for CC2 and CC5 were d=0.574 and d=0.588, respectively, representing a medium effect. (See Fig. 2.)

3.2. Volume

Significant group differences (Wilk's Lambda, F=3.23; p=0.013) were identified for the overall model. Neither age nor sex had a significant effect within the overall model. Bonferroni-corrected individual region contrasts were significant only for region 2 (F=5.57, p=0.022) and region 5 (F=4.94, p=0.030). The effect sizes for CC2 and CC5 were d=.666 and d=1.30, respectively, representing a medium to large effect.

4. Discussion

The present study used the Hofer-Frahm parcellation scheme to examine structural abnormalities in the CC, particularly in middle and posterior regions. With the use of area and volume as indices of CC morphology, our findings confirmed recent reports of mid (Bora et al., 2011; Li et al., 2011) and posterior anomalies (Rosenberg et al., 1997; Garibotto et al., 2010; Park et al., 2010). Specifically, we found significant structural decreases in CC2 and CC5 in OCD patients relative to healthy controls. These regions held significance after controlling for total CC area, total CC volume, and correcting for multiple comparisons for both structural measurements. We did not find significant effects of age, sexual dimorphism, or an interaction of the two in either the area or volume measurements. Unlike previous reports (MacMaster et al., 1999; Saito et al., 2008; Nakamae et al., 2011), we did not find significant differences in the anterior body between OCD patient and healthy controls.

Our first finding points to abnormalities in the CC2, a midbody region composed of axons connecting right and left premotor cortices (PMC) and supplementary motor areas (SMA;Hofer and Frahm., 2006). These medio-frontal regions play an important role in the planning of movement and inhibitory control – behaviors central to cognitive and motor compulsions (Fitzgerald et al., 2010). Several studies have implicated these CC2-linked regions in OCD psychopathology and pathophysiology. For example, Yucel et al. (2007) combined functional MRI and proton magnetic resonance spectroscopy to demonstrate that

OCD patients exhibited elevated activity in the medio-frontal cortex during behavioral suppression. This hyperactivation may help explain the difficulties that OCD patients face when attempting to cease compulsive behaviors. Similar findings were reported in another study that used structural MRI to examine cortical volume in OCD patients and controls. Koprivova et al. (2009) found volumetric decreases in the medio-frontal cortex and dorsocortical areas and suggested these regions to be biomarkers of OCD pathology.

Our study also presents evidence for structural abnormalities in the CC5, the posterior-most segment of the CC. Previous reports of aberrant splenium structure have linked pathology to abnormalities in parietal, temporal, and occipital areas of the cortex (Park et al., 2010). In fact, several studies have found functional and structural abnormalities in these cortical regions in OCD patients using various imaging techniques including voxel-based MRI (Kim et al., 2001), functional MRI (Sanematsu et al., 2010), and DTI (Menzies et al., 2008).

Conversely, our results present some differences in the directionality of callosal pathology. Using structural MRI, Rosenberg et al. (1997) also identified abnormalities along the body of the CC, including CC2 and CC5. However, they found increased area of all segments of the CC except CC4, whereas we found decreases in both area and volume in only CC2 and CC5. Differences in patient and control populations may account for some of these differences. The study of Rosenberg et al. included scans obtained from a medication free pediatric population, whereas we examined a medicated adult population. This difference underscores two influential factors on CC structure: the effects of chronicity of illness and the influence of medication. Since both variables have been shown to alter CC structure (De Luca et al., 2011; Kwon et al., 2009), it is likely that discrepancies in findings may not only be due to different time points within the developmental process of the CC, but also to the changes that occur in the presence of chronic pathology and/or psychotropic drugs. In a medicated adult population similar to ours, Park et al. (2010) found increased area in only CC5. This leads us to suspect that other factors such as differences in segmentation schemes (i.e. functionally guided vs. geometrically based schemes), data analysis (i.e. controlling vs. failure to control for total CC size), or other unforeseen confounds may have also brought forth variability in directionality and regional CC pathology. Interestingly, these inconsistencies in directionality of CC morphology echo those seen in related disorders such as Tourette’s Syndrome (Baumgardner et al., 1996; Kerstin et al., 2006).

Our study presents several limitations that must also be considered. First, our small sample size and wide age range may have hindered our power to identify group differences. To account for these limitations, we calculated the main effects of statistically significant regions of the CC and controlled for age. Secondly, medical and behavioral intervention may have influenced our findings, especially since these factors were not accounted for in our analyses. Given the many reports of neuroanatomical alterations resulting from pharmacotherapy (Kwon et al., 2009) and psychotherapeutic interventions (Roffman et al., 2005), we cannot discount the influences that treatment may have had on brain morphology. Finally, recent research has suggested that the heterogeneous nature of OCD may be related to differences in neurobiological expressions. This may also explain the inconsistent reports of brain morphology and activity in OCD (van den Heuvel et al., 2009;Gilbert et al., 2009). Our failure to measure and control for these dimensions makes it difficult to disentangle

callosal pathology as a general biological marker of OCD or a marker specific to a particular dimension of the disorder.

As the first study to the Hofer-Frahm parcellation scheme on volumetric measurements of the CC in OCD patients, our findings lend strongest support to (1) abnormal morphology of the CC, particularly in the mid-anterior region, and (2) anomalous mid-anterior structure as a likely indicator of premotor cortex and supplementary motor area dysfunction. Future studies utilizing direct measures of connectivity to ascertain medio-frontal pathology may help elucidate the link between the CC2 and premotor areas in the pathophysiology of OCD. The use of functionally guided parcellation schemes, the control of proper covariates (i.e. medication, comorbidity, total CC size), and the consideration of symptom dimensions may allow for better discernment of structural anomalies in the CC and its relationship to cortical pathology. In conclusion, morphological abnormalities in the CC2 support the CC as a neurobiological marker of OCD.

References

Baumgardner TL, Singer HS, Denckla MB, Rubin MA, Abrams MT, Colli MJ, Reiss AL. Corpus callosum morphology in children with Tourette syndrome and attention deficit hyperactivity disorder. Neurology. 1996; 47(2):477–482. [PubMed: 8757024]

Baxter LR Jr. Schwartz JM, Mazziotta JC, Phelps ME, Pahl JJ, Guze BH, Fairbanks L. Cerebral glucose metabolic rates in nondepressed patients with obsessive–compulsive disorder. American Journal of Psychiatry. 1988; 145(12):1560–1563. [PubMed: 3264118]

Bora E, Harrison BJ, Fornito A, Cocchi L, Pujol J, Fontenelle LF, Velakoulis D, Pantelis C, Yücel M. White matter microstructure in patients with obsessive–compulsive disorder. Journal of Psychiatry and Neuroscience. 2011; 36(1):42–46. [PubMed: 21118658]

De Luca V, Gershenzon V, Burroughs E, Javaid N, Richter MA. Age at onset in Canadian OCD patients: mixture analysis and systematic comparison with other studies. Journal of Affective Disorders. 2011; 133(1-2):300–304. [PubMed: 21546093]

Fabri M, Polonara G, Mascioli G, Salvolini U, Manzoni T. Topographical organization of human corpus callosum: an fMRI mapping study. Brain Research. 2010; 1370:99–111. [PubMed: 21081115]

Fitzgerald KD, Stern ER, Angstadt M, Nicholson-Muth KC, Maynor MR, Welsh RC, Hanna GL, Taylor SF. Altered function and connectivity of the medial frontal cortex in pediatric obsessive–compulsive disorder. Biological Psychiatry. 2010; 68(11):1039–1047. [PubMed: 20947065]

Fontenelle LF, Mendlowicz MV, Versiani M. The descriptive epidemiology of obsessive–compulsive disorder. Progress in Neuropsychopharmacology and Biological Psychiatry. 2006; 30(3):327–337.

Friedlander L, Desrocher M. Neuroimaging studies of obsessive–compulsive disorder in adults and children. Clinical Psychology Review. 2006; 26(1):32–49. [PubMed: 16242823]

Garibotto V, Scifo P, Gorini A, Alonso CR, Brambati S, Bellodi L, Perani D. Disorganization of anatomical connectivity in obsessive compulsive disorder: a multi-parameter diffusion tensor imaging study in a subpopulation of patients. Neurobiology of Disease. 2010; 37(2):468–476. [PubMed: 19913616]

Gilbert AR, Akkal D, Almeida JR, Mataix-Cols D, Kalas C, Devlin B, Birmaher B, Phillips ML. Neural correlates of symptom dimensions in pediatric obsessive–compulsive disorder: a functional magnetic resonance imaging study. Journal of the American Academy of Child and Adolescence Psychiatry. 2009; 48(9):936–944.

Hofer S, Frahm J. Topography of the human corpus callosum revisited–comprehensive fiber tractography using diffusion tensor magnetic resonance imaging. Neuroimage. 2006; 32(3):989–994. [PubMed: 16854598]

Kang DH, Kim JJ, Choi JS, Kim YI, Kim CW, Youn T, Han MH, Chang KH, Kwon JS. Volumetric investigation of the frontal-subcortical circuitry in patients with obsessive–compulsive disorder. Journal of Neuropsychiatry and Clinical Neuroscience. 2004; 16(3):342–349.

Kim JJ, Lee MC, Kim J, Kim IY, Kim SI, Han MH, Chang KH, Kwon JS. Grey matter abnormalities in obsessive-compulsive disorder: statistical parametric mapping of segmented magnetic resonance images. The British Journal of Psychiatry. 2001; 179:330–334. [PubMed: 11581113]

Koprivova J, Horacek J, Tintera J, Prasko J, Raszka M, Ibrahim I, Hoschl C. Medial frontal and dorsal cortical morphometric abnormalities are related to obsessive–compulsive disorder. Neuroscience Letters. 2009; 464(1):62–66. [PubMed: 19666084]

Kwon JS, Jang JH, Choi JS, Kang DH. Neuroimaging in obsessive–compulsive disorder. Expert Review of Neurotherapeutics. 2009; 9(2):255–269. [PubMed: 19210199]

Li F, Huang X, Yang Y, Li B, Wu Q, Zhang T, Lui S, Kemp GJ, Gong Q. Microstructural brain abnormalities in patients with obsessive–compulsive disorder: diffusion-tensor MR imaging study at 3.0 T. Radiology. 2011; 260(1):216–223. [PubMed: 21474704]

MacMaster PF, Keshavan MS, Dick EL. Corpus callosal signal intensity in treatment-naïve pediatric obsessive–compulsive disorders. Progress in Neuropsychopharmacology Biological Psychiatry. 1999; 23(4):601–612.

Menzies L, Williams GB, Chamberlain SR, Ooi C, Fineberg N, Suckling J, Sahakian BJ, Robbins TW, Bullmore ET. White matter abnormalities in patients with obsessive–compulsive disorder and their first-degree relatives. American Journal of Psychiatry. 2008; 165(10):1308–1315. [PubMed: 18519525]

Nakamae T, Narumoto J, Sakai Y, Nishida S, Yamada K, Nishimura T, Fukui K. Diffusion Tensor Imaging and tract-based spatial statistics in obsessive–compulsive disorder. Journal of Psychiatric Research. 2011; 45(5):687–690. [PubMed: 20965515]

Nordahl TE, Benkelfat C, Semple WE, Gross M, King AC, Cohen RM. Cerebral glucose metabolic rates in obsessive–compulsive disorder. Neuropsychopharmacology. 1989; 2(1):23–28. [PubMed: 2803479]

Oh JS, Jang JH, Jung WH, Kang DH, Choi JS, Choi CH, Kubicki M, Shenton ME, Kwon JS. Reduced fronto–callosal fiber integrity in unmedicated OCD patients: a diffusion tractography study. Human Brain Mapping. 2012; 33(10):2441–2452. [PubMed: 21922600]

Park HY, Park JS, Kim SH, Jang JH, Jung WH, Choi JS, Kang DH, Lee JM, Kwon JS. Midsagittal structural differences and sexual dimorphism of the corpus callosum in obsessive–compulsive disorder. Psychiatry Research: Neuroimaging. 2010; 192(3):147–153.

Roffman JL, Marci CD, Glick DM, Dougherty DD, Rauch SL. Neuroimaging and the functional neuroanatomy of psychotherapy. Psychological Medicine. 2005; 35(10):1385–1398. [PubMed: 16164763]

Rosenberg DR, Keshavan MS, Dick EL, Bagwell WW, MacMaster FP, Birmaher B. Corpus callosal morphology in treatment-naive pediatric obsessive–compulsive disorder. Progress in Neuropsychopharmacology and Biological Psychiatry. 1997; 21(8):1269–1283.

Saito Y, Nobuhara K, Okugawa G, Takase K, Sugimoto T, Horiuchi M, Ueno C, Maehara M, Omura N, Kurokawa H, Ikeda K, Tanigawa N, Sawada S, Kinoshita T. Corpus callosum in patients with obsessive–compulsive disorder: diffusion tensor imaging study. Radiology. 2008; 246(2):536–542. [PubMed: 18180336]

Sanematsu H, Nakao T, Yoshiura T, Nabeyama M, Tagao O, Tomita M, Masuda Y, Nakatani E, Nakagawa A, Kanba S. Predictors of treatment response to fluvoxamine in obessive-compulsive disorder: an fMRI study. Journal of psychiatric research. 2010; 44(4):193–200. [PubMed: 19758599]

Scarone S, Colombo C, Livian S, Abbruzzese M, Ronchi P, Locatelli M, Scotti G, Smeraldi E. Increased right caudate nucleus size in obsessive–compulsive disorder: detection with magnetic resonance imaging. Research: Neuroimaging. 1992; 45(2):115–121.

Seltzer, B.; Pandya, DN.; Jasper, HH.; Lepore, F.; Ptito, M. The topography of commissural fibers. In: Lepore, F.; Ptito, M.; Jasper, HH., editors. Two Hemispheres, One Brain. Functions of the Corpus Callosum, 1986. Liss, New York: 1986. p. 47-73.

Szeszko PR, Robinson D, Alvir JM, Bilder RM, Lencz T, Ashtari M, Wu H, Bogerts B. Orbital frontal and amygdala volume reductions in obsessive–compulsive disorder. Archives of General Psychiatry. 1999; 56(10):913–919. [PubMed: 10530633]

van den Heuvel OA, Remijnse PL, Mataix-Cols D, Vrenken H, Groenewegen HJ, Uylings HB, van Balkom AJ, Veltman DJ. The major symptom dimensions of obsessive–compulsive disorder are mediated by partially distinct neural systems. Brain. 2009; 132(Pt 4):853, 868. [PubMed: 18952675]

Weis S. Morphometry and magnetic resonance imaging of the human brain in normal controls and Down's syndrome. Anatomical Record. 1991; 231(4):593–598. [PubMed: 1838907]

Witelson SF. Hand and sex differences in the isthmus and genu of the human corpus callosum. A postmortem morphological study. Brain. 1989; 112(Pt 3):799–835. [PubMed: 2731030]

Yoo SY, Jang JH, Shin YW, Kim DJ, Park HJ, Moon WJ, Chung EC, Lee JM, Kim IY, Kim SI, Kwon JS. White matter abnormalities in drug-naive patients with obsessive–compulsive disorder: a diffusion tensor study before and after citalopram treatment. Acta Psychiatrica Scandinavica. 2007; 116(3):211–219. [PubMed: 17655563]

Yucel M, Harrison BJ, Wood SJ, Fornito A, Wellard RM, Pujol J, Clarke K, Phillips ML, Kyrios M, Velakouslis D, Pantelis C. Functional and biochemical alterations of the medial frontal cortex in obsessive–compulsive disorder. Archives of General Psychiatry. 2007; 64(8):946–955. [PubMed: 17679639]

Zarei M, Mataix-Cols D, Heyman I, Hough M, Doherty J, Burge L, Winmill L, Nijhawan S, Matthews PM, James A. Changes in gray matter volume and white matter microstructure in adolescents with obsessive–compulsive disorder. Biological Psychiatry. 2011; 70(11):1083–1090. [PubMed: 21903200]

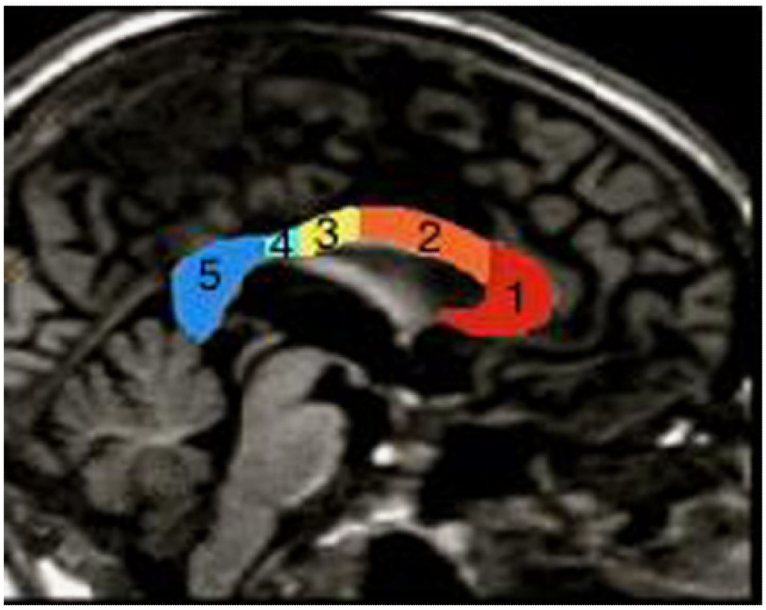

Fig. 1.

Parcellation of the corpus callosum based on the Hofer-Frahm tractography scheme: 1. CC1, 2. CC2, 3. CC3, 4. CC4 and 5. CC5.

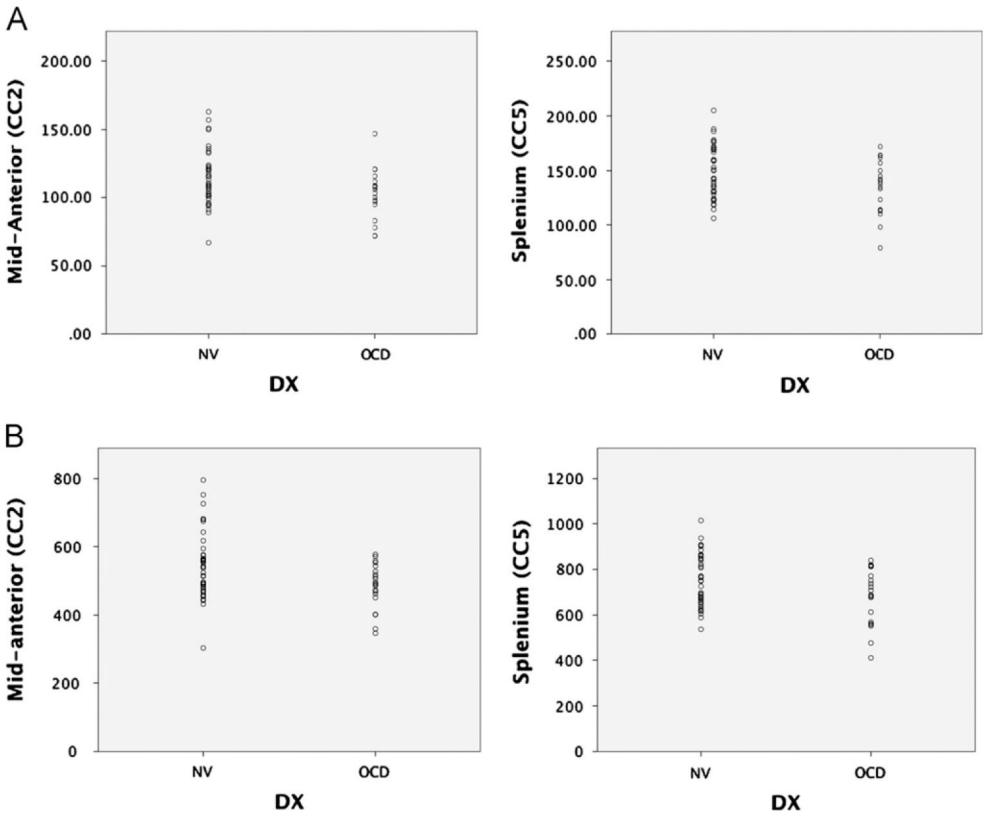

Fig. 2.

Scatterplots representing (A) area (mm^2) and (B) volume (mm^3) measurements of CC2 and CC5 in patients with obsessive–compulsive disorder (OCD) and healthy controls (NV).

Table 1

Summary of studies examining the corpus callosum in obsessive–compulsive disorder.

Author	Year	Sample OCD NV M/F M/F	Medication	Design	Scheme	Findings in OCD group	CC region
Rosenberg et al.	1997	13/8 13/8	Treatment naive	Structural MRI	Witelson	Increased area	Genu (CC1), Anterior (CC2), Posterior (CC3), Splenium (CC5)
MacMaster et al.	1999	13/813/8	Treatment naive	Signal intensity	Witelson	Signal intensity reductions	Genu (CC1)
Saito et al.	2008	7/9 7/9	13 on medication	DTI	Witelson	FA reductions	Rostrum (CC1)
Garibotto et al.	2010	15/0 16/0	13 on medication	DTI	Not specified	FA reductions	Splenium (CC5)
Oh et al.	2012	13/7 13/6	5 on medication	DTI	Brodmann ROI and tract parameterization	FA reductions	Anterior portions of the CC (CC1)
Park et al.	2010	45/24 45/24	16 on medication	Structural MRI	Weis	Increased area	CC1, CC2, CC5
Bora et al.	2011	11/10 14/15	10 on medication	DTI	Not specified	FA reductions	Mid-body of the CC (CC 2, 3, 4)
Li et al.	2011	16/7 16/7	13 on medication	DTI	Not specified	Increased FA	Genu (CC1) and body of the CC (CC2)
Nakamae et al.	2011	14/16 15/15	4 weeks drug-free	DTI	Not specified	FA reductions	Anterior body (CC1)
Zarei et al.	2011	14/12 15/12	16 on medication	DTI	Not specified	Increased FA	Genu (CC1) and splenium (CC5)

CC: corpus callosum; DTI: diffusion tensor imaging; FA: fractional anisotropy; MRI: magnetic resonance imaging; ROI: region of interest

Table 2

Demographic characteristics in obsessive–compulsive patients.

	OCD patients (*N*=21)
Age mean (SD)	26.9 (9.93)
Sex (male/female)	9/11
Handedness (L/R)	4/17
IQ mean (SD)	108 (14)
Medication	
- SSRI *N* (%)	13 (62)
- Tricyclic *N* (%)	3 (14)
- MAOI *N* (%)	1 (5)
- Anxiolytic *N* (%)	5 (24)
- Other *N* (%)	1 (5)
- None *N* (%)	4 (19)

Note: Data are presented as mean (SD). OCD: obsessive-compulsive disorder; SSRI: selective serotonin reuptake inhibitor; MAOI: monoamine oxidase Inhibitor.

Table 3

CC Structure in OCD and healthy controls using manual tracings.

	OCD patients (*N*=21)	Controls (*N*=42)	*F*	*P*
CC1 (Genu)	115.76 (22.24)[a]	117.50 (20.50)[a]	0.100[a]	0.753[a]
	578.86 (101.41)[b]	592.90 (104.20)[b]	0.250[b]	0.619[b]
CC2 (Mid-anterior)	103.74 (17.66)[a]	115.05 (21.04)[a]	4.62[a]	0.036*[a]
	485.29 (64.83)[b]	539.93 (96.05)[b]	5.57[b]	0.023*[b]
CC3 (Mid-posterior)	44.19 (9.08)[a]	46.93 (10.15)[a]	1.11[a]	0.296[a]
	216.10 (40.75)[b]	226.67 (45.98)[b]	0.779[b]	0.381[b]
CC4 (Isthmus)	19.38 (4.51)[a]	21.93 (5.99)[a]	2.87[a]	0.095[a]
	97.81 (20.58)[b]	108.45 (28.70)[b]	2.26[b]	0.138[b]
CC5 (Splenium)	134.57 (23.89)[a]	148.62 (23.52)[a]	4.83[a]	0.032*[a]
	679.38 (121.15)[b]	748.98 (113.30)[b]	4.95[b]	0.030*[b]

Note: Dataset using age and sex as covariates. Data are presented as mean (S.D.).

[a] Area.

[b] Volume.

* $P<0.05$.